

Design of Silicon-Based Leaky-Mode Resonant Nanopatterned Devices Using Inverse Numerical Methods

M. Shokooh-Saremi^{*}, R. Magnusson^{*}, T. J. Suleski^{**} and E. G. Johnson^{**}

^{*}Department of Electrical Engineering, University of Texas at Arlington, USA
saremi@uta.edu, magnusson@uta.edu

^{**}Center for Optoelectronics and Optical Communications, Department of Electrical & Computer Engineering, University of North Carolina at Charlotte, USA
egjohnso@uncc.edu

ABSTRACT

The objective of this research is design of nanophotonic resonance devices including filters, mirrors, and polarizers with minimal materials requirements. Thus, single-layer, silicon-based, two-dimensional resonant leaky mode elements implemented with periodic waveguide layers are presented. We apply particle swarm optimization to design these devices. Example results include a broadband reflector with center wavelength of 1700 nm and bandwidth of ~ 161 nm across which the zero-order reflectance exceeds 99%. An efficient bandpass filter with spectral width of ~ 2 nm at 1550 nm central wavelength is realized. The versatility of the leaky-mode resonance concept is rendered clearly as these single-layer devices consist of identical materials yet provide completely different spectral expressions. Particle swarm optimization is thus effective for this class of problems and straightforward in implementation.

Keywords: particle swarm optimization, leaky-mode resonance, guided-mode resonance, diffraction grating.

1 INTRODUCTION

Resonant leaky-mode (guided-mode) elements have recently drawn much attention and shown high capability for being utilized as functional photonic devices [1]. Leaky waveguide modes can be excited when an incident light beam is coupled into the waveguide structure through an inscribed periodicity under phase-matching conditions. This results in generation of a guided-mode resonance field response in the spectrum [2]. Device operation can be explained in terms of the photonic band structure and associated leaky-wave effects near the second stop band [3]. Resonant devices such as biosensors, tunable filters, display pixels, polarizers, bandpass filters, and wideband reflectors can be realized using this operational principle.

The electromagnetic resonance response and associated leaky-mode field interactions are very complex in this class of devices. Therefore, to realize the desired spectral response, it is essential to apply efficient design/optimization methods that find the device parameters yielding the desired result. To that end, we show

here that particle swarm optimization (PSO) is a useful design tool. PSO is a robust, stochastic evolutionary strategy recently applied in electromagnetic design problems [4,5].

In this work, we present new 2D-nanopatterned silicon-based guided-mode resonance devices operating in the 1.5-2.0 μm spectral region. The aim of this research is realization of compact, low-loss photonic elements for use as laser cavity reflectors and bandpass filters. Using PSO, we design polarization-independent, single-layer (silicon on glass) devices by 2D patterning. Future experimental realization and comparison with theory is planned.

2 LEAKY-MODE RESONANCE BASICS

Diffraction gratings are well-known elements with numerous applications in optics and optical engineering. In one of their special classes, gratings are fabricated over optical waveguides, mainly as a light coupler, or patterned over a substrate as both light guide and coupler. In these types of elements, an incident light beam, upon satisfying the grating/waveguide's phase-matching condition, can excite waveguide leaky modes. These modes can be reradiated through the same grating structure to the incident and substrate media. This results in generation of a guided-mode resonance (GMR) field response in the spectrum [2]. This spectral signature in its basic form is a very sharp reflection or transmission peak. Figure 1 illustrates resonance interactions between the leaky waveguide and an incident plane wave. At short wavelengths, as the grating has low spatial frequency with respect to the incident wave, there exist propagating orders other than the zero orders (multi-order regime). As the wavelength increases, the propagation angles of the higher-order waves increase. Eventually, all the higher-order waves will become evanescent, or cut off, and the high-efficiency zero-order regime (or subwavelength regime) prevails. Figure 2 displays two basic, one-dimensional (1D) GMR structures. The structure displayed in Fig. 2(b) is particularly simple as it consists merely of a single patterned layer.

The grating structural parameters including period, thickness, and fill factor, as well as the refractive indices of the grating materials and the surrounding media, angle of incidence, and polarization influence the shape and

behavior of the resonance response. The grating parameters generally define the resonance wavelength and location and the refractive index contrast in the grating region strongly affects the spectral width [6]. The physical basics of operation of these elements can be understood by studying the associated photonic band structure especially near the second (leaky) stop band [3]. Photonic devices with a variety of spectral properties are achievable upon proper placement and manipulation of the resonance peaks at the second stop band [1]. Figure 3 shows a typical band structure (dispersion diagram) of a GMR element

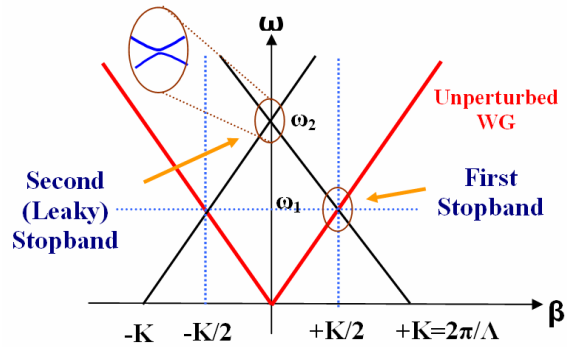


Figure 3: Illustration of a typical band structure (dispersion diagram) of a GMR element. This element operates near the second (leaky) stopband in which $\beta = K$. β is the propagation constant of the mode, K is the grating constant ($K = 2\pi/\Lambda$, Λ is the grating period), and ω is the angular frequency.

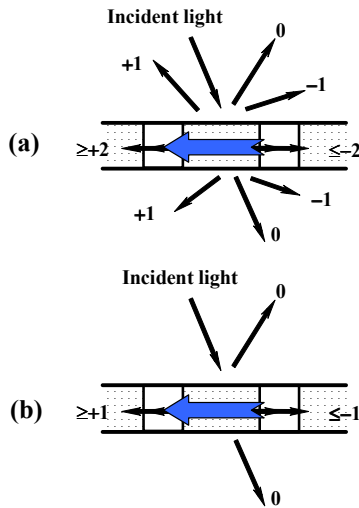


Figure 1: Interaction between a periodic waveguide and an incident plane wave. (a) Excitation of a leaky mode in a higher-order diffraction regime. (b) Excitation of a leaky mode in the zero-order (subwavelength) diffraction regime.

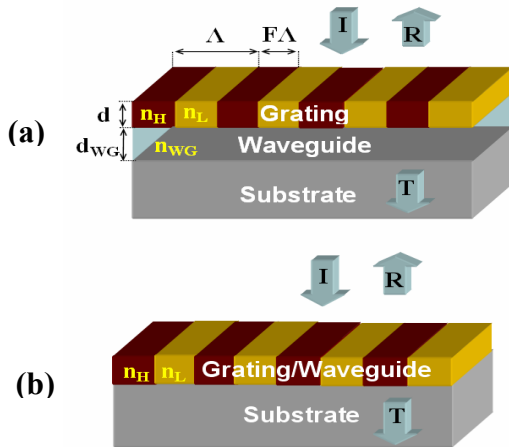


Figure 2: Schematics of two basic 1D GMR structures. (a) Grating acting as a light coupler for the waveguide underneath. (b) Grating functioning as both coupler and light guiding medium. The second structure is often applied on account of its simplicity. Λ , d , d_{WG} , and F are period, grating thickness, waveguide thickness, and fill factor (fraction of period with higher refractive index), respectively.

In this paper, we will design elements with two-dimensional periodicity (2D GMR as in [7]), which have more analysis complexity than the 1D GMRs, however, the electromagnetics basics of both are the same. 2D GMR elements can exhibit special spectral and polarization-dependent or independent features. The 2D GMR structure treated will be introduced in section 4.

3 PARTICLE SWARM OPTIMIZATION

Particle swarm optimization (PSO) is a robust, stochastic evolutionary strategy that has recently been utilized in electromagnetic design problems [8]. This method, introduced by Eberhart and Kennedy [4], is inspired from social behavior of animal species like birds, bees and others (“particles”) for finding their requirements in the search area. The algorithm finds the optimal solution by moving the particles in the search space. Because of the convenience of realization and promising optimization capability in various problems, PSO is of growing interest to researchers. PSO lets every individual within the swarm move from a given point to a new one with a velocity based on a weighted combination of the individual’s current velocity, best position ever found by that individual, and the group’s best position. In this paper, a standard PSO algorithm is introduced and then applied to the design of guided-mode resonance filters [5].

In PSO, each particle of a swarm is considered as a point in an N -dimensional search space, which adjusts its movement according to its own experience as well as the experience of other particles. Each particle is represented by an N -parameter vector given by

$$\mathbf{X}_m = \{x_{1m}, x_{2m}, \dots, x_{Nm}\} \quad 1 \leq m \leq N_{POP} \quad (1)$$

where m is an integer and indicates the position of the particle in the swarm, which has N_{POP} particles. For numerical evaluation of the quality of particles, a fitness

function (FF) is defined and determined for each particle according to its optimization parameters. The algorithm initiates by randomly locating particles moving with random velocities. Velocity is the rate of a particle's position change and is represented by $\mathbf{V}_m = \{v_{1m}, v_{2m}, \dots, v_{Nm}\}$. The fitness function is calculated for all particles in the initial swarm. The best previous particle position (Pbest) is set initially to the initial particle position, $\mathbf{P}_m = \{p_{1m}, p_{2m}, \dots, p_{Nm}\}$, and the position of the best particle in the swarm (Gbest) is kept as the swarm's best position (\mathbf{G}).

The modification of the particle's position in (k+1)th iteration can be modeled as follows:

$$\mathbf{V}_m^{k+1} = w\mathbf{V}_m^k + c_1 \text{rand}_1()(\mathbf{P}_m - \mathbf{X}_m^k) + c_2 \text{rand}_2()(\mathbf{G} - \mathbf{X}_m^k) \quad (2)$$

$$\mathbf{X}_m^{k+1} = \mathbf{X}_m^k + \mathbf{V}_m^{k+1} \Delta t \quad (3)$$

where w is the inertia weight, c_1 and c_2 are called cognitive and social rates, respectively, and $\text{rand}_1()$ and $\text{rand}_2()$ are two uniformly distributed random numbers between 0 and 1. Equation 2 shows that the new particle's velocity has memories of the previous velocity, its own best position and the best position of the swarm. The position of each particle is then updated according to Eq. 3, in which Δt is the time step (here $\Delta t = 1.0$). Also, \mathbf{P}_m and \mathbf{G} are updated based on the following rules:

- \mathbf{P}_m update rule:

If $FF(\mathbf{X}_m^{k+1})$ is better than $FF(\mathbf{P}_m)$ then $\mathbf{P}_m = \mathbf{X}_m^{k+1}$.

- \mathbf{G} update rule:

If best of $FF(\mathbf{P}_m, 1 \leq m \leq N_{POP})$ is better than $FF(\mathbf{G})$ then

$\mathbf{G} = \text{best of } \mathbf{P}_m (1 \leq m \leq N_{POP})$.

The iterations continue, by returning to calculation of Eqs. (2) and (3), until either an optimum solution is obtained or the maximum number of iterations is met.

4 DESIGN RESULTS

Using PSO, we design polarization-independent, single-layer (silicon on glass) devices based on 2D GMR concepts, operating in the 1.5-2.0 μm spectral region. Grating thickness (d), period ($\Lambda = \Lambda_x = \Lambda_y$), and fraction of period with refractive index of n_H ($F = F_x = F_y$) are the optimization parameters; see Fig. 4. Therefore, $\mathbf{X} = \{\Lambda, d, F\}$ is the particle (filter) structure. θ , δ , ψ , and the refractive indices of incidence (n_{inc}), substrate (n_{sub}), and grating (n_H, n_L) media are set to proper values in each example. A standard PSO scheme, as summarized in section 3, is utilized to synthesize filters with a desired spectral response (Target). The number of particles in the swarm (N_{POP}) is fixed to 20. Cognitive (c_1) and social (c_2) rates are set to 1.49 and inertia weight (w) decrease linearly from 0.9 to 0.4 through iterations (maximum number of iterations is set to 10,000). An absorbing boundary condition is utilized to limit the search in the predetermined search space [8]. The

fitness function (FF) is considered to be an RMS error function:

$$FF = \left\{ \frac{1}{M} \sum_{\lambda_i} [R_{desired}(\lambda) - R_{design}(\lambda)]^2 \right\}^{1/2} \quad (4)$$

in which $R_{desired}(\lambda)$ is the desired filter reflectance and $R_{design}(\lambda)$ is its PSO-designed counterpart (in case of bandpass filters, transmittance (T) is employed). Here, M is the number of wavelength points (λ_i). Rigorous coupled-wave analysis (RCWA) is used for diffraction efficiency calculations [7,9].

Figure 4 shows the design model, which is a 2D GMR element. The input wave can be either normally or conically incident on the 2D patterned silicon layer; here we consider the case of normal incidence. Also, in our design examples, we set $\Lambda_x = \Lambda_y$ and $F_x = F_y$, hence the spectral response of element is the same for TE ($\psi = 90^\circ$) and TM ($\psi = 0$) polarizations. The examples presented illustrate the versatility of the approach in a single layer. Here, we use simple patterning, namely two parts (silicon/air) per period. Using several parts per period can substantially increase the quality of the sought solutions; the price for this enhancement is that finer nanoscale patterning would be required. This is a topic for future work in 2D photonic lattices.

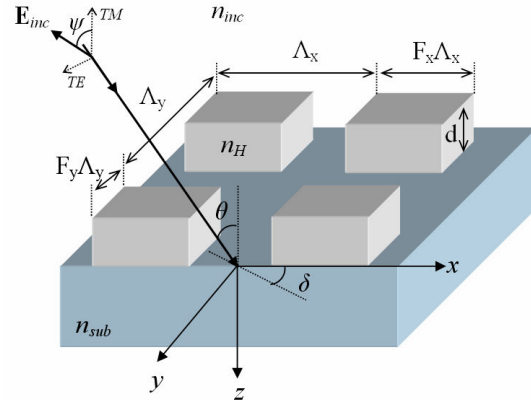


Figure 4: Design model for 2D GMR devices. Λ_i and F_i are periods and fill factors in azimuthal directions (i: x, y). θ , δ , and ψ are incidence, azimuthal, and polarization angles, respectively.

Figure 5 shows the spectral response of a narrow-band reflector over the 1500-1600 nm wavelength band. This subwavelength, single-layer, silicon-on-silica structure with optimized parameters provides reflection bandwidth ~ 3 nm (full-width at half-maximum: FWHM) centered at 1550 nm. The fixed parameters of this design are: $n_H = 3.48$, $n_{inc} = 1.0$, $n_{sub} = 1.48$, $\theta = \delta = 0^\circ$, and $\psi = 90^\circ$. The optimal design parameters found by PSO are: $\Lambda_x = \Lambda_y = 738.7$ nm, $F_x = F_y = 0.672$, and $d = 854.6$ nm.

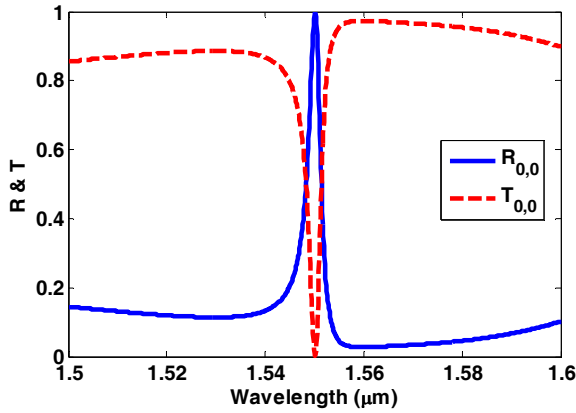


Figure 5: Reflectance and transmittance of a narrow-band reflector. The parameters of this device are: $\Lambda_x = \Lambda_y = 738.7$ nm, $F_x = F_y = 0.672$, $d = 845.6$ nm, $n_H = 3.48$, $n_{inc} = 1.0$, $n_{sub} = 1.48$, $\theta = \delta = 0$, and $\psi = 90^\circ$. The bandwidth is ~ 3 nm (FWHM).

Figure 6 illustrates the spectral response of a broadband reflector over the 1500-2000 nm band. This structure with optimized parameters provides reflection bandwidth of ~ 161 nm ($R_{0,0} > 0.99$). This element can be employed for example as a laser cavity mirror.

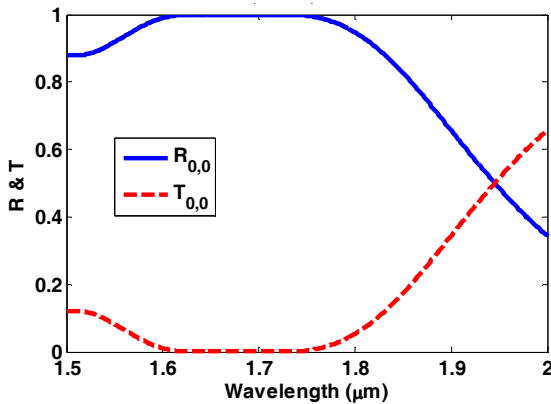


Figure 6: Reflectance and transmittance of a broadband reflector. The parameters of this device are: $\Lambda_x = \Lambda_y = 869.6$ nm, $F_x = F_y = 0.543$, $d = 585$ nm, $n_H = 3.48$, $n_{inc} = 1.0$, $n_{sub} = 1.48$, $\theta = \delta = \psi = 0^\circ$. The reflection bandwidth of this mirror is ~ 161 nm ($R_{0,0} > 0.99$).

Figure 7 shows the response of a narrow bandpass (transmission) filter in the 1500-1600 nm band. The spectral width of this filter is ~ 2.0 nm (FWHM) centered at 1550 nm.

Design and optimization of GMR elements in two-dimensions is well suited for inverse numerical methods. The examples provided here show the capability of the PSO technique (even in its simplest form) in design and optimization of 2D GMR elements with a variety of reflection and transmission spectral responses.

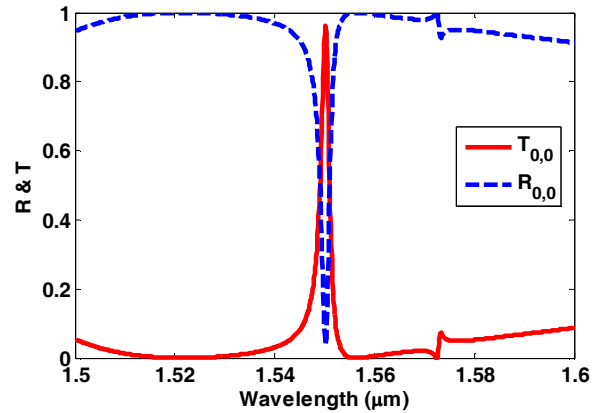


Figure 7: Spectral response of a narrow bandpass filter. The parameters of this device are: $\Lambda_x = \Lambda_y = 840.8$ nm, $F_x = F_y = 0.861$, $d = 578.2$ nm, $n_H = 3.48$, $n_{inc} = 1.0$, $n_{sub} = 1.48$, $\theta = \delta = 0$, and $\psi = 90^\circ$. The bandwidth of the filter is ~ 2 nm (FWHM) with central wavelength of 1550 nm.

5 CONCLUSIONS

In this paper, a variety of two-dimensional guided-mode resonance elements with desired spectral responses (narrow-band and broadband reflectors, and a narrow bandpass filter) are designed. A standard particle swarm optimization technique is utilized as design/synthesis method. It is shown that PSO is a powerful technique for designing 2D GMR elements that is one of the challenging problems in this field.

REFERENCES

- [1] Y. Ding and R. Magnusson, *Opt. Express* 12, 5661-5674, 2004.
- [2] S. S. Wang and R. Magnusson, *Appl. Opt.* 32, 2606-2613, 1993.
- [3] Y. Ding and R. Magnusson, *Opt. Express* 15, 680-694, 2007.
- [4] R. Eberhart and J. Kennedy, "Particle swarm optimization," in *Proc. IEEE Conf. on Neural Networks*, 1942-1948, 1995.
- [5] M. Shokooh-Saremi and R. Magnusson, *Opt. Lett.* 32, 894-896, 2007.
- [6] D. Shin, S. Tibuleac, T. A. Maldonado and R. Magnusson, *Opt. Eng.* 37, 2634-2646, 1998.
- [7] S. Peng and G. M. Morris, *J. Opt. Soc. Am. A* 13, 993-1005, 1996.
- [8] J. Robinson and Y. Rahmat-Samii, *IEEE Tran. Antennas Propagat.* 52, 397-407, 2004.
- [9] T. K. Gaylord and M. G. Moharam, *Proc. IEEE* 73, 894-937 (1985).